

Fluid dynamics in clouds: The sum of its parts

S. Ravichandran,^{1,*} Jason R. Picardo,^{2,†} Samriddhi Sankar Ray,^{3,‡} and Rama Govindarajan^{3,§}

¹*Nordita, KTH Royal Institute of Technology and Stockholm University, Roslagstullsbacken 23, 10691 Stockholm, Sweden*

²*Department of Chemical Engineering, Indian Institute of Technology Bombay, Mumbai 400076, India*

³*International Centre for Theoretical Sciences, Tata Institute of Fundamental Research, Bangalore 560089, India*

This paper is aimed at describing cloud physics with an emphasis on fluid dynamics. As is inevitable for a review of an enormously complicated problem, it is highly selective and reflects of the authors' focus. The range of scales involved, and the relevant physics at each scale is described. Particular attention is given to droplet dynamics and growth, and turbulence with and without thermodynamics.

I. GLOSSARY

Aerosol: tiny ($\sim 0.1 - 1$ micron) solid particles suspended in the air. There are about 100-1000 aerosol particles per cubic centimeter of air.

Clouds: mixtures of air ($\sim 99\%$ by weight), water vapour (1%), liquid water droplets (0.1%), aerosol particles, trace gases. Clouds are usually in turbulent flow.

Caustics: regions of the flow where particles with different velocities arrive simultaneously at the same location.

Supersaturation: a system that has more water vapour than the saturation value prescribed by the Clausius-Clapeyron equation 5.

Ventilation effects: the effects of oncoming flow on the growth of droplets. Used in the context of water droplets growing by condensation.

II. WHY STUDY CLOUDS

Clouds, since they involve many different phenomena interacting with each other in complex ways, are of interest purely from scientific curiosity. For instance, is it possible to predict what cloud shapes will result for given atmospheric conditions? More importantly, perhaps, clouds are also immensely influential in the energy and mass balances in the planet's atmosphere. In fact, clouds are the last great sources of uncertainty in climate science.

Clouds increase the planet's albedo, reflecting away sunlight before it can make it to the surface; they also act to provide a greenhouse effect, trapping energy radiated away from the surface. These two opposing effects are both of much larger magnitudes than any other sources in the radiative balance of the planet ([4] chapter 6, [99]). The response of clouds to a warming planet—whether clouds will act to slow down or to accelerate the planet's warming—is not clear at present (although very recent

studies ([91]) suggest that they do indeed act as positive feedback). This uncertainty is due to the large magnitudes of the aforementioned effects, and the fact that clouds are coupled with the global circulation.

The selective annual Northward propagation of the cloud-band known as the ITCZ (Inter-Tropical Convergence Zone) over longitudes including those of the Indian landmass, brings the Indian monsoon, among the biggest weather events, which provides fresh water for close to two billion people. Understanding the dynamics of the ITCZ requires understanding the dynamics of clouds, which is as yet an open problem ([20]). These are only a few of the most compelling reasons to study clouds.

With the advent of machine learning and associated statistical and data-driven techniques, and the increasing availability of dedicated computing power, it is tempting to rely solely on such statistical methods. However, understanding the dynamics is useful not just as a scientific exercise but also pragmatically. Statistical techniques—machine learning in particular—are best used in scenarios for which they have been 'trained'. Most estimates suggest that the feedback from clouds on the climate is likely to affect the circulation in the atmosphere substantially. The resulting large changes in the dynamics may not be possible to capture with machine learning techniques. The planet needs us to study the dynamics of clouds! ([90].)

III. DEFINITION OF THE SUBJECT

The fluid dynamics in clouds covers length scales from tenths of microns to hundreds of kilometres. Being a nonlinear problem, the physics at each scale has an effect on other scales. There are open questions which require an understanding of the basic physics at each scale, and also in the connections between scales. The lower end of this range concerns the chemistry and chemical physics of aerosols. Aerosols are crucial to cloud formation, because they act as nuclei for droplet formation, as will be discussed below. Aerosols are introduced into the atmosphere in a variety of ways, natural and anthropogenic. The production of aerosols, especially sea-salt

* ravichandran@su.se

† jrpicardo@che.iitb.ac.in

‡ samriddhisankarray@gmail.com

§ rama@icts.res.in

aerosol by the mechanics of wave-breaking at the surface of the ocean, is an outstanding problem of fluid mechanics. The upper end of the range of length scales covers the dynamics of weather and the climate. Significant progress has been made in recent years, aided by advances in supercomputing, in the ability to make reasonable predictions of the dynamics on these scales. The robustness of these predictions depends, however, on understanding the global dynamics at the ‘sub-grid scales’. The intermediate range, incorporating the interactions of buoyancy-driven fluid turbulence of (dilute) suspensions, is not only exceedingly complex, but also controls the dynamics of processes at the largest scales related to weather and climate. We will describe recent progress in understanding the dynamics in the intermediate length scales.

Studies of the cloud dynamics can be based on observations of clouds either in the real world or in the laboratory, or on analyses or numerical solutions of the fluid dynamical equations of motion. Our work is in the latter, and we will for the most part restrict ourselves to discussing theoretical/ numerical studies of clouds, although we do make note of some relevant experimental studies.

An important ingredient in the intermediate scales is that clouds are usually in turbulent flow. Turbulence consists of vortices and regions of shear whose length scales span a large range, starting from the biggest scale in a single cloud, of the order of a few kilometres, to what is known as the Kolmogorov scale η , which is of the order of a millimetre in a cloud. A turbulent flow is characterised, among other properties, by its Reynolds number, which is a ratio of inertial and viscous forces. Consider a cloud of length scale $L \sim 1$ kilometre in height and width, where velocities U are of the order of 10m/sec. The kinematic viscosity ν of air is about $10^{-5} \text{m}^2/\text{sec}$. The Reynolds number is $LU/\nu \sim 10^9$.

The range of length scales involved even within the intermediate range in clouds is vast. Accurate direct numerical simulations (DNSs), solving the Navier-Stokes equations or their variants, have to resolve the Kolmogorov scales of turbulence. If these scales have to be resolved in simulations of a cloud of the length scale of 100m, each dimension has to be resolved with $O(10^5)$ grid points. Such numerical simulations are impossible with today’s computing resources. DNSs of cloud flows are typically conducted only within small boxes, of a few metres in length [57–59]. In other words a small volume within a cloud is all we can simulate. In effect experiments (on a computer or in the laboratory) can be performed at Reynolds numbers that are much smaller than those found in clouds, in the hope that this will nevertheless provide useful answers [1, 26–28, 66, 70, 71, 80, 93, 108] at cloud Reynolds numbers (see also section VB1). Workarounds for this limitation take the form of large eddy simulations (LESs) which resolve only the large scales of motion (i.e. they are ‘cloud-resolving’) [39, 51, 77, 84] and use models to account for

the smaller scales including the microphysics of phase-change.

The radius a of a typical water droplet in a cloud ranges from about a micron to a few millimetres. Obviously even simulations that resolve the Kolmogorov scales of the flow cannot resolve the scales associated with the motion of the water droplets in clouds. Even the simplest approach to tracking droplets adds significantly to the burden of computations, given that there are $O(1000)$ small droplets per cubic centimetre of cloud. In the simplest approach, the finite-sized water droplets have to be treated as point particles and tracked in a Lagrangian sense. Alternatively, these particles can be coarse-grained into a field. The relative efficacies of these two approaches to particle-dynamics are studied in [64]. The effects of finite droplet size and how this changes their dynamics is discussed at length in section IV. These are known as “one-way coupled” approaches, where the fluid equations are solved for without taking into account the fact that fluid is carrying particles and droplets, whereas the dynamics of the particles and droplets are dictated by the fluid motion. For a dilute suspension of small particles and droplets this is a fair approach. However, larger raindrops can affect the flow and can affect the dynamics of each other, and a perfect treatment would have to account for the forces of these objects on the fluid and on each other (two-way or four-way coupling). This can make computational costs forbidding.

The thermodynamics taking place within a cloud has an important effect on the dynamics. Phase change results in heat release, which results in buoyancy. The potential energy thus gained is converted into the kinetic energy of turbulence. Thus turbulence in a cloud is fundamentally different from mechanically forced turbulence, and turbulence from heat supplied at the boundaries, which are studied most often. We return to this point in section VA. The droplet-growth bottleneck is a well-known open problem. Droplets can grow quickly to about 10 microns in size in a supersaturated environment typical of clouds. Once they are about 50 microns in diameter, gravity can aid in the process of droplet growth by enhancing collision probability, with some fraction of all collisions resulting in coalescence. How droplets grow from about 10 to about 50 microns is not completely understood yet, and this is known as the droplet-growth bottleneck. Turbulence is widely accepted now to be a big part of the answer, and this is discussed below.

Most present-day studies assume that water droplets are spherical in shape whereas larger drops are sensitive to gravity and can distort in shape from the spherical, even to the point where they adopt shapes which are locally sheet-like, which then causes breakup into smaller droplets. Ice crystals are most often not spherical. Thus, the roles of shape, surface tension, gravity and even surface chemistry on the dynamics have to be studied. These effects are also important in the thermodynamics of water droplet growth (discussed in section VA) and in the collisions-coalescence of water droplets (section IV).

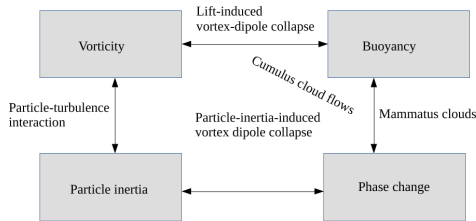


FIG. 1. Cloud dynamics as the sum of its components.

Another important attribute is that over the length-scales that clouds occupy in the atmosphere, air is a compressible fluid. Note that the Earth’s atmosphere at a height of ten kilometres is only a tenth as dense as it is on the ground. So a parcel of air, as it rises, will undergo significant expansion, which cannot be neglected by assuming incompressibility. The equations of compressible fluid motion are significantly more complicated than those of an incompressible fluid (which itself is a “Millennium problem”). The fully compressible equations of motion for air contain sound waves which operate on very short timescales. These sound waves are unimportant for the dynamics of interest to us and computing them would require short timesteps and greatly increase the computational requirements. Fortunately, since the Mach numbers Ma associated with the flow are small, the thermodynamic pressure of the ambient can be decoupled from the pressure fluctuations due to the motion (which are $O(Ma^2)$ relative to the thermodynamic means). This allows the use of the anelastic equations for flows over large heights or the incompressible equations for shallow flows, the latter of which is the limit we are concerned with. A sketch of the derivation of the anelastic and incompressible equations from the compressible equations may be found in [5, 34]. As the name suggests, the anelastic equations ‘filter out’ the sound waves from the dynamics, leaving only the effects of compressibility on the large scale dynamics. On relatively small scales, the assumption of incompressibility is reasonable and is typically made in studies of the flows in shallow clouds [70, 71, 93, 108], and even in some idealised studies of deep convection [47].

As we see in figure 1, the dynamics of clouds is an interplay of particle inertia, thermodynamics, the resulting buoyancy driven flow. At the largest scales, the effect of Earth’s rotation, and solar radiation and its modification by clouds, need to be understood better, and we do not deal with these topics in the present paper.

In summary, studies at different scales have to sometimes be carried out in isolation, using approaches and assumptions appropriate for that scale. New physics is revealed at each scale, and their effects must then be included in our studies at other scales.

IV. MICROPHYSICS WITHOUT THERMODYNAMICS

A simple framework, which ignores the effects of thermodynamics, phase changes and the associated changes in temperature, to understand the physics of a *single* warm cloud is to model it as a dilute suspension of small, spherical water droplets of radius a which are advected by a statistically stationary, homogeneous and isotropic, full-developed turbulent flow. Such an approach ignores the effect of condensation, arising from a super-saturated environment, by assuming that the starting point of such studies are non-precipitating droplets which are already condensed to sizes of about $10\mu m$; hence further growth through condensation over a reasonably short time window, corresponding to the life-time of such a cloud, is unlikely [18, 31, 41, 61, 95].

Such a simplification has at least two distinct advantages. Firstly, it allows us to formulate and address questions of collisions, coalescences, and gravitational settling (precipitation) in the turbulent setting of a cloud in a precise way. Secondly, given this framework, it lends itself easily to the use of tools and ideas developed in the field of turbulent transport over the last two decades or so.

In typical clouds, given $a/\eta \ll 1$, the Reynolds number associated with a droplet $Re_p \ll 1$. This allows us to define the dynamics of a droplet, in the presence of a gravitational force \mathbf{g} and an (turbulent) advecting fluid velocity \mathbf{u} , in terms of its position \mathbf{x}_p and velocity \mathbf{v} , through the linearised Stokes drag model with a Stokes time τ_p [81]:

$$\frac{d\mathbf{x}_p}{dt} = \mathbf{v}; \quad (1a)$$

$$\frac{d\mathbf{v}}{dt} = -\frac{\mathbf{v} - \mathbf{u}(\mathbf{x}_p)}{\tau_p} + \mathbf{g}. \quad (1b)$$

The velocity field of the carrier flow, driven to a statistically steady state through a force \mathbf{f} , with density ρ_f , a kinematic viscosity ν , and a pressure field P , satisfies the incompressible, three-dimensional Navier-Stokes equation

$$\frac{\partial \mathbf{u}}{\partial t} + (\mathbf{u} \cdot \nabla) \mathbf{u} = \nu \nabla^2 \mathbf{u} - \frac{\nabla P}{\rho_f} + \mathbf{f}; \quad (1c)$$

$$\nabla \cdot \mathbf{u} = 0. \quad (1d)$$

Given the assumptions of a small droplet and a dilute suspension, the underlying flow is assumed to be unaffected by the presence of such water droplets.

The effect of the finite size and the density contrast of the particle with the carrier flow, which leads to a finite time of relaxation of the particle velocities to that of the fluid, is captured by the Stokes time $\tau_p = \frac{2a^2\rho_p}{9\nu\rho_f}$, where the particle density is given by ρ_p ; for clouds (water droplets in air), the ratio of these two densities is $\rho_p/\rho_f \sim 1000$. However, it is useful to measure this inertia of the particles in terms of the non-dimensional Stokes

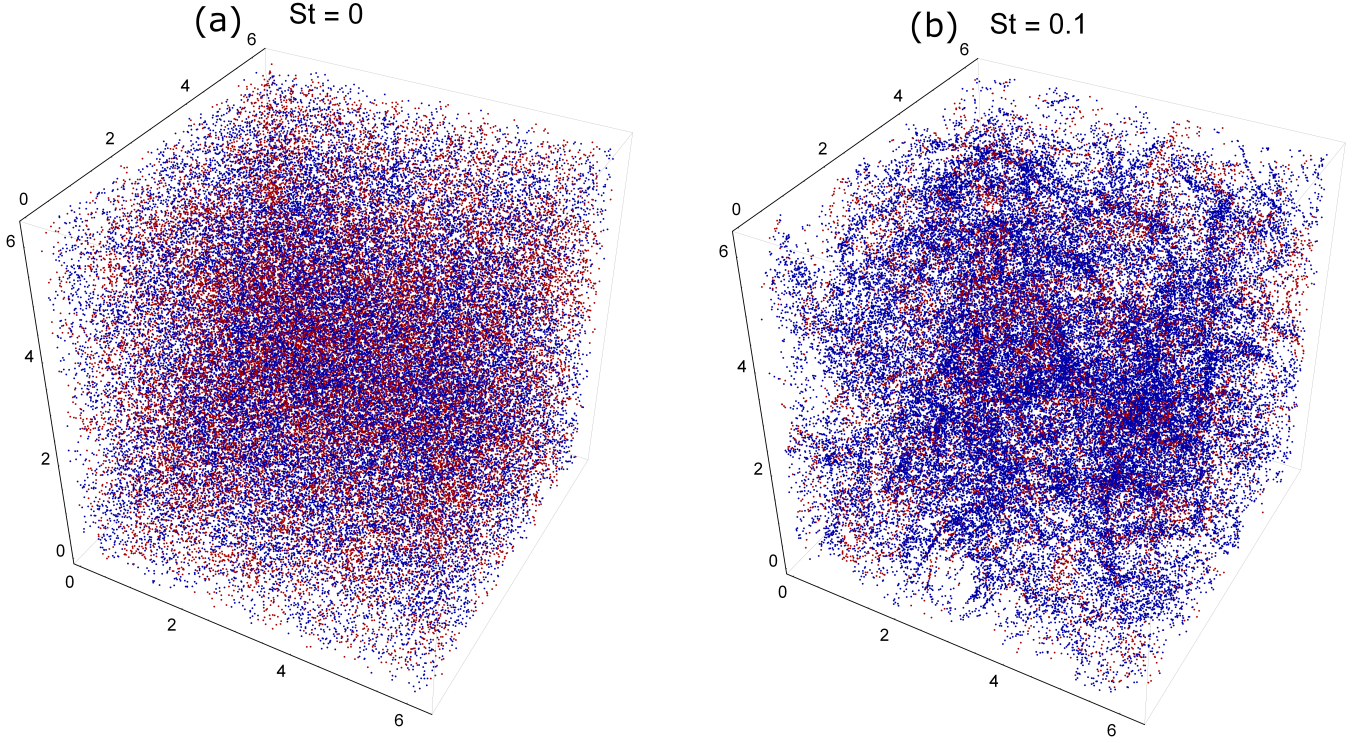


FIG. 2. Snapshots of tracers (a) and inertial particles (b), with $St = 0.1$, in a three-dimensional turbulent flow. Particles in regions dominated by rotation ($\mathcal{Q} > 0$) are colored red, while those in regions dominated by straining ($\mathcal{Q} < 0$) are colored blue. The dissipative dynamics of inertial particles ($St = 0.1$) causes them to form dynamic clusters, which are seen in panel (b) to mainly reside in straining regions, in accordance with the ejection of inertial particles from rotational zones.

number $St = \tau_p/\tau_\eta$, where $\tau_\eta = \sqrt{\nu/\epsilon}$ is the characteristic, short-time, Kolmogorov time-scale of the fluid (ϵ is mean energy dissipation rate). Such non-dimensional numbers allow an easy comparison between observations, experiments, theory and numerical simulations.

The linear Stokes drag model (Eqs. 1a-1b) is, of course, in the heavy-particle limit $\rho_p \gg \rho_f$, a simplification of the Maxey-Riley equation [62] for the motion of a spherical particle (with $Re_p \ll 1$) in a flow:

$$\rho_p \frac{d\mathbf{v}}{dt} = \rho_f \frac{D\mathbf{u}}{Dt} + (\rho_p - \rho_f)\mathbf{g} - \frac{9\nu\rho_f}{2a^2} \left(\mathbf{v} - \mathbf{u} - \frac{a^2}{6} \nabla^2 \mathbf{u} \right) - \frac{\rho_f}{2} \left(\frac{d\mathbf{v}}{dt} - \frac{D}{Dt} \left[\mathbf{u} + \frac{a^2}{10} \nabla^2 \mathbf{u} \right] \right) - \frac{9\rho_f}{2a} \sqrt{\frac{\nu}{\pi}} \int_0^t \frac{1}{\sqrt{t-\xi}} \frac{d}{d\xi} (\mathbf{v} - \mathbf{u} - \frac{a^2}{6} \nabla^2 \mathbf{u}) d\xi \quad (2)$$

where $\frac{D}{Dt}$ denotes the full convective derivative and it factors in the effects of the force due to the undisturbed flow $\rho_f \frac{D\mathbf{u}}{Dt}$, the buoyancy $(\rho_p - \rho_f)\mathbf{g}$, the Stokes drag $\frac{9\nu\rho_f}{2a^2} \left(\mathbf{v} - \mathbf{u} - \frac{a^2}{6} \nabla^2 \mathbf{u} \right)$, the added mass $\frac{\rho_f}{2} \left(\frac{d\mathbf{v}}{dt} - \frac{D}{Dt} \left[\mathbf{u} + \frac{a^2}{10} \nabla^2 \mathbf{u} \right] \right)$, and the Basset history $\frac{9\rho_f}{2a} \sqrt{\frac{\nu}{\pi}} \int_0^t \frac{1}{\sqrt{t-\xi}} \frac{d}{d\xi} (\mathbf{v} - \mathbf{u} - \frac{a^2}{6} \nabla^2 \mathbf{u}) d\xi$ effects. Without going into a rigorous demonstration of how Eq. 2 reduces to Eq. 1b, we can immediately see that for heavy particles the force due to the undisturbed flow is negligible and the only effect of gravity is a net acceleration downwards. Furthermore, the Faxen corrections $\sim a^2 \nabla^2 \mathbf{u}$ for small particles are negligible as is the Basset term in such

dilute suspensions of passive particles. (On the last aspect, we refer the reader to a recent work by Prasath *et al.* [75] for a detailed analysis of the Basset history term). Indeed recent work by Saw *et al.* [88] have confirmed by comparing experimental data with those obtained from a numerical simulation of Eqs. 1, that the approximation discussed here are indeed reasonably valid for the dilute suspensions of small, but heavy, particles that we consider in this paper.

Before we proceed further, it might be useful at this stage to comment on how Eqs. 1 are solved on the computer [22]. (See Ref. [69] for a discussion on the nature of such simulations in two-dimensional flows.) The incompressible Navier-Stokes equations (Eqs. 1c-1d)

are typically solved, in three dimensions, on a tripe-periodic 2π cube with N^3 collocation points; in the results being reviewed in this paper, N has ranged from 512 up to 2048 yielding Taylor-scale based Reynolds number which range from (approximately) 120 to 450. The flow is driven to a statistically steady, homogeneous and isotropic, turbulent state with an external forcing. There is of course considerable freedom in the way we choose to force the fluid; two particularly popular choices are one with a constant energy injection as low wave-numbers [89] and another where (again at low wavenumbers) a second-order Ornstein–Uhlenbeck process [60] is adapted to provide a more *random* forcing. The equations themselves are solved through a standard pseudo-spectral method where spatial derivatives are taken in Fourier space to allow an easy integration in time of what essentially becomes an algebraic equation.

Solving for the particle dynamics (Eqs. 1a-1b) are less involved. The only non-trivial element in this is to use suitable interpolation schemes to obtain the fluid velocity, which is calculated on a regular Eulerian grid, at typically off-grid particle positions. Several such schemes exist and the ones commonly used are the cubic spline, the B-spline, the trilinear, or the cubic interpolation schemes (see e.g. [104]).

The consequences of the linear Stokes drag model have been studied extensively [8, 9, 23, 45, 48, 65] since the pioneering work of Bec [6, 7]. A detailed discussion of this is certainly beyond the scope of this present paper. However, in what follows, it is useful to recall two central features of the dynamics defined by Eqs. 1, namely *preferential concentration* and *caustics*.

The dissipative dynamics of the particle motion leads to a preferential sampling of the flow and hence a preferential concentration of particles as opposed to a homogeneous distribution in the flow (as seen for tracers) for finite Stokes numbers: Particles with finite sizes evolve to (dynamically changing) attractors with fractal dimensions. Traditionally, this preferential concentration or inhomogeneities in the distribution of particles is captured through the correlation dimension D_2 obtained from calculating the probability $P^<(r)$ of two particles being within a distance r , whence $P^<(r) \sim r^{D_2}$. The correlation dimension D_2 is of course a function of the Stokes number St . In the limit of vanishing St (tracers), particles must distribute homogeneously and hence, in a three-dimensional flow, $D_2 = 3$. For very large values of St , the motion of particles are essentially decorrelated from the flow and thus have a more ballistic behaviour. This results, yet again, in space-filling and consequently $D_2 = 3$. At intermediate values of St , however, the particles distributions are inhomogeneous $D_2 < 3$ and maximal clustering (or inhomogeneities) is observed (with an accompanying minimum in D_2) for $St \sim \mathcal{O}(1)$. We refer the reader to Figs. 1 and 2 in Ref. [9] for an illustration of these effects.

From the perspective of flow structures, the clustering of heavy inertial particles can be tied to their ejection

from vortical or rotational regions of the flow. One way to quantify this behaviour is via the \mathcal{Q} -criterion [33], which uses the local velocity gradient matrix \mathcal{A} to define a quantity $\mathcal{Q} \equiv (R_{ij}^2 - S_{ij}^2)/2$ (where $R = (\mathcal{A} + \mathcal{A}^T)/2$ and $S = (\mathcal{A} - \mathcal{A}^T)/2$). Regions dominated by rotation (straining) have $\mathcal{Q} > 0$ (< 0). Fig. 3(a) presents the Lagrangian probability distribution functions (PDFs) of \mathcal{Q} measured along the trajectories of tracers and inertial particles with various values of St . The undersampling of vortical regions by inertial particles is clearly visible; indeed the effect is significant even for St as small as 0.03 (relevant for 10 – 20 μm cloud droplets). This effect gets stronger upto $St \approx 0.5$, beyond which the particles begin to decorrelate from the underlying flow structures, until eventually, for large St , the PDF approaches that for tracers (cf. $St = 8.3$ in Fig. 3(a)).

The fact that ejection from vortices leads to concentration and clustering in straining regions is shown clearly in Fig. 3(b), which presents a coarse-grained particle number density (using cubic bins of side 20η), conditioned on the local value of \mathcal{Q} , and for various St . As St increases from zero, the density of particles in regions of moderate straining increases, while the density in rotational regions reduces. This is illustrated visually by Fig. 2(b), wherein most of the dense particle clusters are blue ($\mathcal{Q} < 0$). Fig. 3(b) also shows that particle density reduces with St in regions of very high straining, indicating that inertial particles cannot cluster in such intense regions of the flow, but rather prefer mildly straining zones.

A second important ingredient in this story is caustics [78]. Caustics are defined here as regions in the flow where droplets of different velocities can arrive simultaneously at the same location. In other words, caustics are regions of the flow where droplet velocity cannot be described as a field. These are significant for the following reason. Droplets of moderate Stokes number (~ 0.1 to 1) get ejected quickly out of vortices, and this increases their propensity to collide and coalesce, but smaller droplets are usually taken to behave like passive scalars, just advecting passively with the flow. Under this assumption no preferential concentration takes place for small droplets, and collisions would be extremely rare. We thus do not have a mechanism by which small droplets can coalesce and begin to cross the bottleneck. In the immediate vicinity of a single vortex of circulation Γ , i.e., within a distance $\sim \sqrt{\Gamma\tau_p}$ from the vortex centre, even the smallest droplets are centrifuged out [78], and caustics can form. It was shown [30, 78] that collisions between small droplets can be greatly enhanced in the caustics region, giving rise to a small number of droplets which can cross the bottleneck, and become the seeds for further coalescence events.

Given this context, let us return once more to questions within the framework of turbulent transport which are pertinent to the problem of droplet dynamics in a warm cloud. In particular, the questions that we discuss in this paper have to do with collisions, coalescences, and precipitation. Specifically these are best discussed by an-

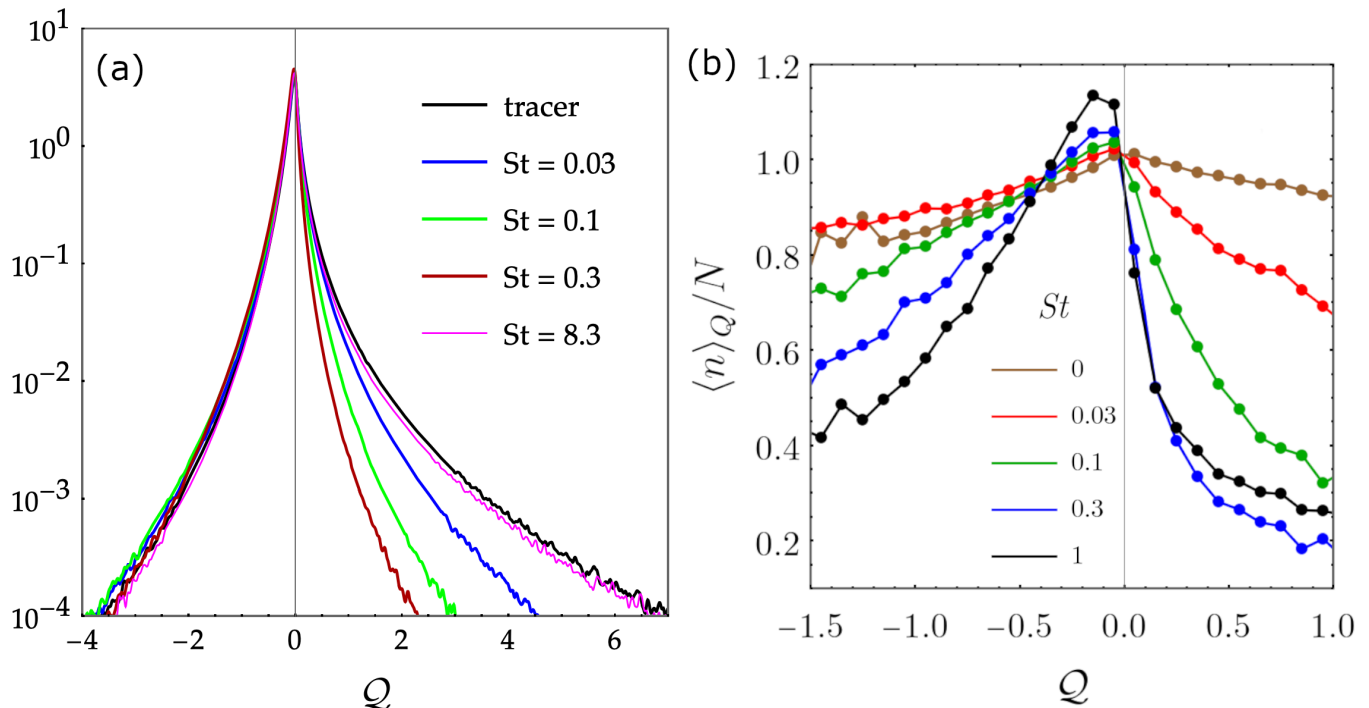


FIG. 3. Panel (a) presents PDFs of Q sampled by tracers and inertial particles with various values of St . Panel (b) shows the average coarse-grained particle number density, conditioned on the local value of Q , for various St .

swering the following questions: How fast—and where—do droplet collide? How fast do droplets grow (by coalescence)? And, how fast do droplet settle under gravity? (The issue of the structure of such aggregates when they collide, but not coalesce, will not be covered in this overview [11, 42].)

Turbulence is thought to play a dominant role in enhancing the droplet-droplet collision rates, and in turn the droplet-size distributions as well as the initiation time of rain, in typical warm clouds[36, 95]. The underlying mechanism instrumental in this is not only preferential concentration, discussed above, but also, through *slings* [14, 36] and *caustics* [35, 109], the extreme velocities with which particles can approach each other. Therefore in order to gain insights which can help build mesoscopic models for collision kernels, it is important to have reliable estimates of the typical relative velocities between droplets which are about to collide in a turbulent flow.

This issue was addressed by Saw *et al.* [88] who, through experiments, numerical simulations and theory, studied the probability distribution functions of the velocity differences between pairs of particles, measured along the line-of-sight, when they are quite close to each other. In the experiment, a turbulent flow was generated within a 1 *m*-diameter acrylic sphere [14] with Taylor micro-scale Reynolds numbers R_λ as high as 190 corresponding to values of η as low as $180 \mu m$. In such a flow, a bi-disperse population of droplets were introduced, via a spinning disc [107], with mean diameters $6.8 \mu m$ and

$19 \mu m$ which are much smaller than η . Given that the experiment was able to achieve three different R_λ , and hence η , it was possible to obtain particle trajectories for 6 different Stokes numbers through stereoscopic Lagrangian Particle Tracking [67]. In the numerical simulations, of the sort described above, particle trajectories were obtained for the similar Stokes numbers and for comparable values of R_λ which allowed a meaningful comparison of theory and experiments.

A convenient measure of the statistics of how droplets impact on each other, is through the probability distribution function of the longitudinal component of the velocity differences v^\parallel between pairs of particles and conditioned on their separation r . In Fig. 1 of Ref. [88], these distribution functions for four different values of the Stokes number and, in each case, conditioned on three different values of the separation r are shown. The agreement between the experimental and numerical data, especially for the larger values of St , is a confirmation of the validity of the linearised Stokes drag model of Eqs. 1. However, it is worth pointing out that these distributions, which seem to fit the form of stretched exponentials [53] and at odds with the compressed exponential prediction for large Stokes numbers [46], show consistently, for reasons still not clear, a greater convergence between the numerical and experimental data for the left tail (approaching pairs) than for the right tail (separating pairs). Furthermore, a closer examination of these distributions show that droplet-pairs approach each other with increasing relative velocities—and a possible increase in collision

rates—as their Stokes number increases consistent with other evidences of the sling effect [14].

These distributions were of course conditioned on small ($\mathcal{O}(\eta)$) but still finite separations; in the context of understanding collisions amongst droplets in a cloud, we should examine the relative velocities at contact or at least when they are even closer to each other ($r \rightarrow 0$). It turns out that all these distributions can be collapsed on top of one another (Fig. 2 in Ref. [88]) by a simple rescaling with r^β ; experimental and numerical data suggests that β has a mild Stokes-dependence and for reasonably large values of St (not entirely valid for droplets in a cloud at its infancy), corresponding to extreme velocity differences, its value is consistent to the saturation exponent ξ_∞ of the higher-order moments of relative velocities [10]. The positive exponent β , which is small for small droplets, nevertheless suggests the possibility of mild impact velocities on contact.

The particle dynamics in a more realistic cloud is of course non-stationary as droplets grow and change their sizes and numbers. A step in this direction is to account for the polydispersity in a suspension. James and Ray [50] investigated this problem for suspensions in two and three-dimensional turbulent flows. Interestingly, the authors were able to derive the typical impact velocities between particle pairs which, in principle, could have different Stokes numbers. This was conveniently done by assuming a reference particle with a Stokes number St_1 and a second one with St_2 ; in the usual mono-disperse problem, $St_2 = St_1$. Assuming the smoothness of the underlying fluid velocity at small inter-particle separations, the impact velocity Δ was theoretically calculated (under suitable approximations) for pairs of droplets with different Stokes numbers and validated against numerical simulations.

As we discussed before, because of the collision-coalescence processes, it is safe to assume that particle dynamics in a cloud may well be non-stationary. As a result of this James and Ray have also looked at the collision rates in a non-stationary phase and found an enhancement of this, when compared to the collision rates in the statistically stationary phase for all non-zero Stokes numbers. Interestingly, this ratio peaks to 2 (Fig. 4 in Ref. [50]) when the Stokes number of the colliding pairs are around 0.2. Although the results obtained suggests a lack of universality, this observation might be one possible explanation of possible run-away processes which explains the rapid growth of droplets from tiny nuclei, seed rain drops. We also refer the reader to recent studies in Refs. [16, 17, 43, 44, 63] on the issue of such poly-disperse suspensions and the relative velocities of colliding inertial particles in turbulent flows.

All of this inevitably leads us to the question of how the size distribution of droplets evolve when we turn on actual coalescences in a suspension advected by a turbulent flow. A time-honoured theoretical framework for studying such problems is the Smolochowski's equation with a stationary coalescence rate or kernel. Starting with

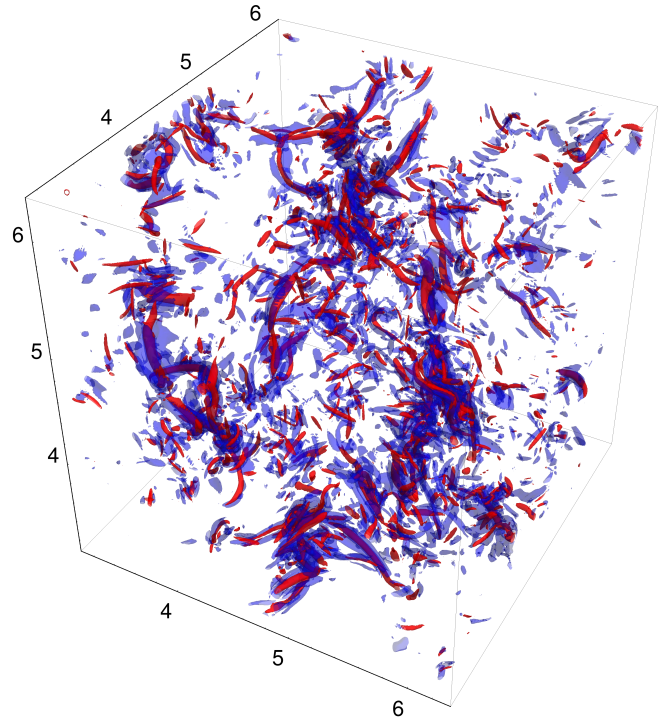


FIG. 4. Snapshot of intense rotational (red) and straining (blue) regions in a turbulent flow, visualized using the Q -criterion. Intense vortical/rotational regions take the form of tubes or *worms* that are enveloped by strongly straining sheet-like structures, forming vortex-strain wormrolls. Reproduced from [74].

an initial infinite bath of particles of the same size (and mass), such an approach inevitably leads to a growth in the population of droplets of large sizes as a simple power-law in time. Specifically, assuming an initial infinite bath of particles of mass 1, the number of particles with mass i (also, in these units, an integer since coalescence imposes mass conservation) grows as

$$n_i(t) \simeq n_1^i (t/t_i)^{i-1}. \quad (3)$$

(The time t_i appearing in the exponent is taken as an average time-scales set by the different stationary collision rates between all particle pairs which add up to give the i -th particle).

However, when such particles are in a dilute suspension carried by a turbulent flow, how accurate are these estimates emerging from Smolochowski's equation? This question was answered, through a combination of theory and numerical simulations, by Bec *et al.* in Ref. [13]. This work carefully analysed the contribution to the coalescence rate coming not from the microphysics of adhesion but the fact that particles are in a turbulent flow. This non-trivial contribution was shown to factor in the anomalous part δ_3 in the scaling of the third-order structure function in a turbulence-advected passive-scalar field $\langle (\theta(\mathbf{x} + \mathbf{r}) - \theta(\mathbf{x}))^3 \rangle \sim |\mathbf{r}|^{1-\delta_3}$ and leads to a population

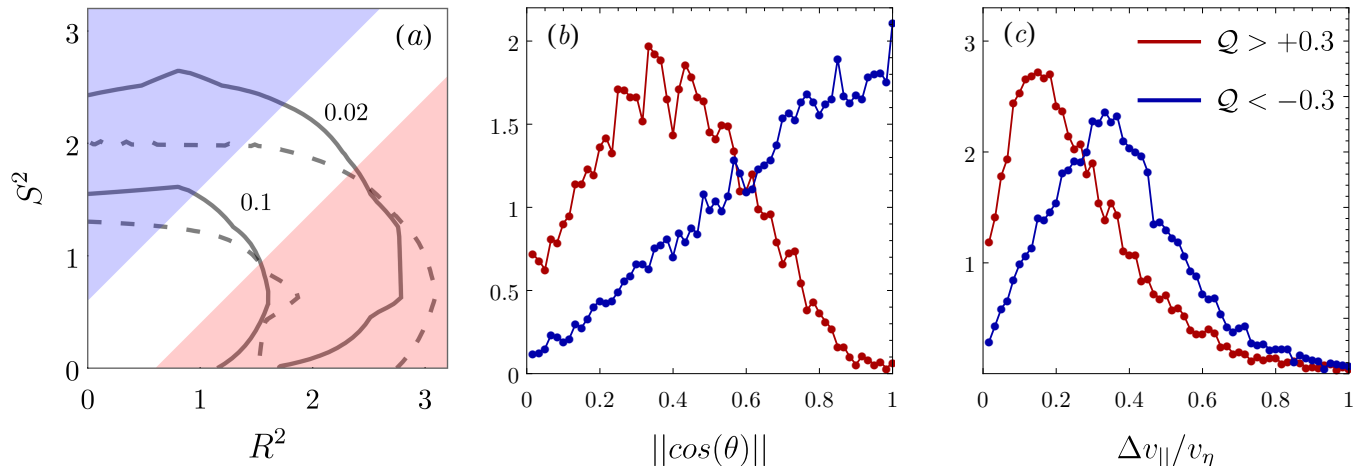


FIG. 5. Panel (a) presents the 0.1 and 0.03 level contours of the joint probability distribution function of the values of R^2 and S^2 , measured at the positions of inertia-less ($St = 0$) particles (dashed) and at their collision locations (solid). Panels (b) and (c) present distributions of the collision angles and the collision velocities, respectively, conditioned on whether the collisions occur in rotational ($Q > +0.3$, red) or straining ($Q < -0.3$, blue) regions. The contribution of these regions to the joint distribution in panel (a) is shown by the red/blue shading. Taken together, these panels show that collisions in straining regions tend to occur in a head-on or rear-end fashion, which results in a higher collision approach velocity, and thereby a higher collision frequency. Reproduced from [74].

growth of the form

$$n_i(t) \simeq n_1^i (t/\tilde{t}_i)^{(1-\frac{3}{2}\delta_3)(i-2)+1}. \quad (4)$$

Given that the (universal) value of $\delta_3 \approx 0.18$, this form suggests a more rapid growth of droplets with masses different from the bath of monomers of mass 1.

The accuracy and correctness of the theoretical calculations were benchmarked against state of the art direct numerical simulations with an initial suspension of 1 billion monomers which were then allowed to coalesce and form droplets of other sizes in the same paper [13]. Figure 2 in this work shows the accuracy of the prediction (4) at early times; a further confirmation of the importance of anomalous scaling was obtained via the probability density function of the inter-coalescence times between the initial monomers (of mass 1) and other droplets of different sizes which were subsequently formed (Fig. 3 in Ref [13]). Remarkably, these results are perhaps the only ones which show how anomalous scaling in turbulence shows up as a leading order effect in a more applied problem such as the one of coalescences in turbulent transport.

This work thus established a plausible argument to suggest a rapid growth in droplets at short times through a complex (Lagrangian) correlated sequence of events. However the fate of these droplets at long time still remains a large unexplored issue.

All of these measurements are of course central in building up models for collision and coalescences in a warm cloud. However, they do not help us, in a direct way, to uncover the correlation, if any, between collisions and the flow structures peculiar to turbulence. In-

deed, even small-scale, homogeneous and isotropic turbulence, which we may expect to encounter in the core of a cumulus cloud, is rich in structure: It is perforated by a hierarchy of rotational and straining flow structures [25, 32, 52, 94, 97, 110], as shown in Fig. 4. These structures are a physical manifestation of the intermittency of the velocity gradient field, which distinguishes fully-developed turbulence from a simple random Gaussian field [49, 68, 101]. One may ask, therefore, whether the collisions between inertial particles or droplets are sensitive to these flow structures, and thereby to the non-Gaussian nature of turbulence. This question was addressed recently by Picardo et al. [74], who measured the relative values of rotation (R^2) and straining (S^2) at the locations of collisions, and compared them to the values sampled by particle trajectories. They found that collisions among small St particles are disproportionately frequent in straining regions, much more than what may be anticipated from preferential concentration alone. In fact, this effect is not fundamentally tied to inertia, but persists even in the limit of $St \rightarrow 0$, for which the particles are homogeneously distributed. (In this limit, the particles are effectively tracers, but with a small fictional radius that enables the detection of collisions.)

Figure 5(a) presents contours of the joint probability distribution of the values of R^2 and S^2 , measured both where inertia-less particles reside (dashed contours) and where they collide (solid contours). Here, straining (rotational) regions with $Q < -0.3$ ($> +0.3$) are shaded in blue (red). Clearly, there is an oversampling (undersampling) of straining (vortical) regions by collisions, compared with the particle trajectories. This discrepancy is a result of the very different flow geometry

in these regions. Colliding particles in straining regions tend to approach each other in a head-on or rear-end fashion, whereas particles in rotational regions approach each other in a side-on manner and undergo glancing collisions. This is shown by the conditioned-PDFs of the collision angle θ (the angle between the relative velocity and position vectors of the two colliding particles), presented in Figure 5(b). For a given magnitude of the underlying fluid velocity, head-on collisions are faster than side-on collisions, as shown in Figure 5(c), because a larger component of the relative-velocity of the particles is translated into the collision velocity. For the same number density of particles, this results in a higher collision frequency in straining regions.

Particle inertia acts to enhance this preference of collisions for straining regions, upto $St \approx 0.3$. This is seen in Fig. 6(a), which presents the average value of $Q = (R^2 - S^2)/2$ measured at particle and collision locations, as a function of St . At small St , inertia selectively enhances the collision velocity in straining regions, as shown in Fig. 6(b), and therefore increases the frequency of collisions in straining regions relative to rotational regions. At larger values of St , however, the particles begin to decorrelate from the underlying flow structures and both particle and collision locations begin to distribute uniformly (cf. the inset of Fig. 6(a)) and also collide with comparable velocities in straining and vortical regions (Fig. 6(c)). This mismatch between where inertial (for small St) particles reside and collide was earlier observed by Perrin and Jonker [72], who also analyzed the influence of flow structures on collisions using the eigenvalues of the velocity gradient matrix [73], which enable a finer classification of structures than the simple Q -criterion.

We have seen that collisions between small St particles are sensitive to the local underlying structure of the flow. As St approaches unity, however, collisions are affected not just by the structure at the collision location, but by all the flow structures encountered by the particles, upto a time of about τ_p prior to the collision, or upto a distance of $|v|\tau_p$ around the collision. This raises the possibility of intense vortical and straining regions conspiring to generate violent, rapid collisions, due to their peculiar vortex-strain worm-roll geometry (cf. Fig. 4): Particles in intense vortex tubes will be ejected with large slip velocities into the enveloping straining sheets, where they have a high chance of colliding with large relative velocities. Picardo et al. [74] found evidence for this scenario, by Lagrangian backtracking of particles that collided in straining regions: the particles which collided in the least time after being ejected from a vortex, were indeed the ones that originated from the strongest vortices, collided in the strongest straining regions and with the largest collision velocities.

This effect of vortex-strain worm rolls was found to be prominent only for St beyond about 0.5. This value may seem too large for small cloud droplets, and indeed it is when one considers the particle relaxation time rela-

tive to the mean Kolmogorov time-scale of the turbulent flow. However, at the extremely large Re of in-cloud turbulence, there are likely to be a few, very intense, intermittent vortices, with a local flow time scale that is much smaller than the mean Kolmogorov time-scale. This means that local, *effective* St of particles in the vicinity of such intense vortices will be closer to unity, making the vortex ejection and collision scenario relevant. Even if such intense vortices occupy a very small volume fraction of the flow, the rapid collisions generated will be able to act as a seed that initiates the runaway growth of droplets by gravitational driven collision-coalescence [56].

Unfortunately, the Re values that can be directly simulated on a computer are still orders of magnitude smaller than what is expected for a cloud. Therefore, it is not possible to directly investigate the effect of high- Re flow structures. However, one can gain a basic understanding of how such structures may influence the motion and collisions of droplets by using model vortex flows. Such an analysis was carried out in two-dimensions, using point and gaussian vortices, by Ravichandran et al. [78] and Deepu et al. [30], and later extended to a three-dimensional Burgers vortex [21] by Agasthya et al. [2]. These studies show that particles near the core of a strong vortex are ejected more rapidly than particles farther away. This leads to a large increase in the local particle density around the periphery of the vortex (Fig. 3 of [2]), as well as large relative velocities between neighbouring particles (caustics). These factors combine to significantly enhance collisions in the vicinity of the vortex. Figure 7 shows the coarse-grained collision density Θ (obtained from a large ensemble of simulations) as a function of the radial distance r from the axis of a Burgers vortex, which serves as a model for the intense vortex tubes [24, 37] observed in three-dimensional turbulence (cf. Fig. 4) [32, 97]. Three cases are presented, corresponding to a mild, wide vortex ($r_{core} = 0.4$) and an intense thin vortex ($r_{core} = 0.2$), with mild and strong axial straining ($\sigma = 0.08$ and 0.3 respectively). The straining flow along the vortex-axis is seen to enhance the number of collision produced around an intense vortex, by drawing particles in towards the core of the vortex.

Taken together, these results show that collisions are definitely sensitive to the structure of the turbulent flow, and suggest that the intense and intermittent vortex-strain structures, characteristic of turbulence, may play a key role in the coalescence driven growth of droplets in clouds.

Before we conclude this section, let us touch upon briefly the question of how such droplets settle under gravity. The mean settling velocity V_s , i.e., the component of the particle velocity along the direction of gravity, of a particle with a Stokes time τ_p is simply $(1b) V_s = \tau_p g - \langle u_z(\mathbf{x}_p, t) \rangle$. In the absence of a flow or a uniform sampling of the flow by the particles, $\langle u_z(x_p, t) \rangle = 0$ and leading to a predictable settling velocity $V_s = \tau_p g$. However in the presence of a background turbulent flow,

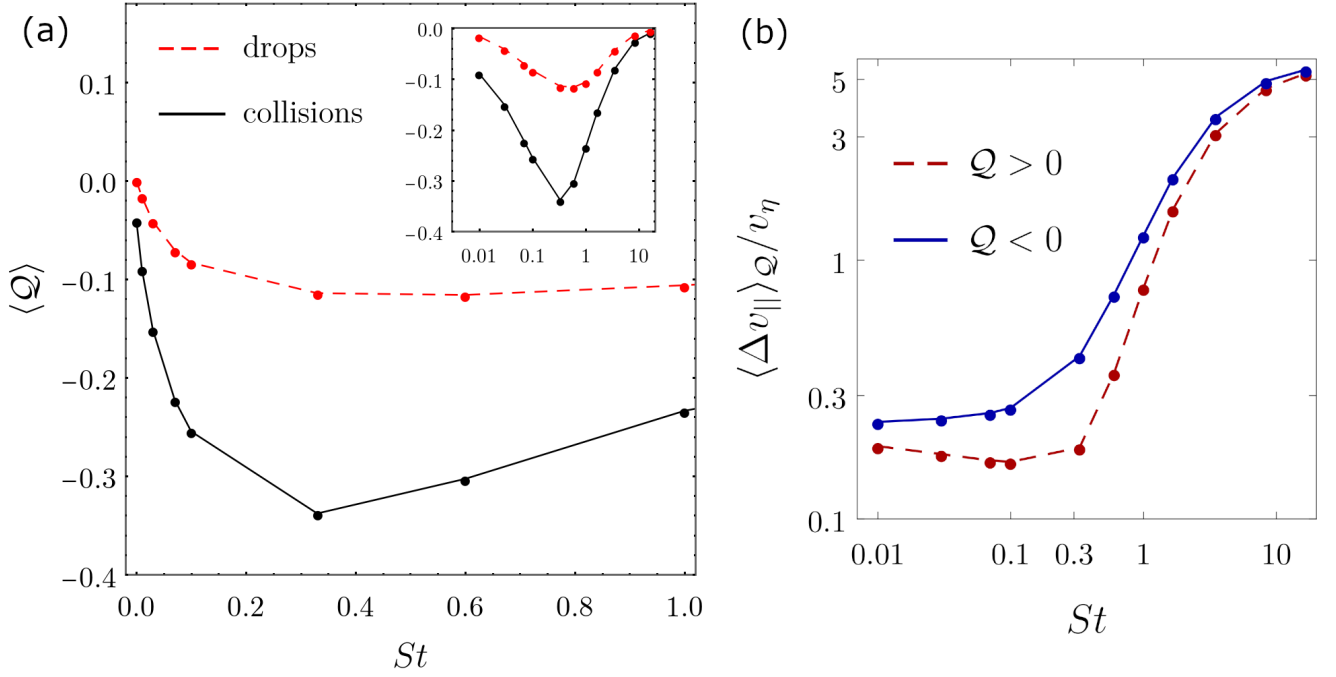


FIG. 6. Panel (a) presents the average value of Q measured where inertial particles or droplets collide (black-solid) and reside (dashed-red), as a function of St . The inset presents the same result for a wider range of St using a semi-log scale. Panel (b) presents the average collision velocity, conditioned on whether collisions occur in regions dominated by rotation (red) or strain (blue), as a function of St . Adapted from [74].

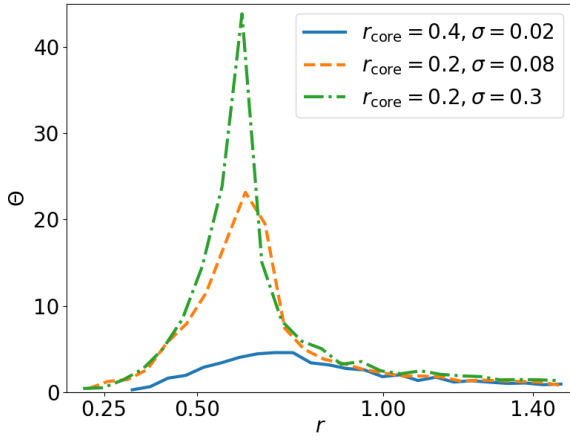


FIG. 7. Coarse-grained collision density Θ , i.e. the number of collision per unit volume, as a function of the radial distance r from the axis of a tubular Burgers vortex. r_{core} is a measure of the size of the core of the vortex, i.e. of how intensely the vorticity is concentrated about the vortex-axis. σ is a measure of the straining flow, that is directed inward along the radial direction and outward along the vortex-axis. This straining is essential for maintaining a concentrated vortex tube in a viscous fluid, where vorticity continuously diffuses outward [24]. Here, we see that this straining flow also acts to enhance the collisions around intense vortices. Reproduced from [2].

it has been known that the settling velocity can be enhanced through an oversampling of the regions where the fluid velocity is downwards. A systematic and quantitative understanding of this phenomenon was carried out by using extensive numerical simulations and theory by Bec *et al.* in Ref. [12].

A convenient way to estimate this enhancement of the settling velocity is to measure the relative increase $\Delta_V = (V_s - \tau_p g) / (\tau_p g) = -\langle u_z(\mathbf{x}_p, t) \rangle / (\tau_p g)$ as a function of the Stokes number. In Fig. 2 of Ref [12], the authors showed the Δ_v is indeed positive and a non-monotonic function of St with a peak at $St \sim 1$. This enhancement, in the limit of small values of St was understood by showing that the correlation $\langle u_z \nabla_\perp \cdot \mathbf{v} \rangle = \tau_p^2 g \langle (\partial_z u_z)^2 \rangle > 0$. This shows that clustering of particles on any horizontal plane (perpendicular to the direction of gravity)—and hence $\nabla_\perp \cdot \mathbf{v} < 0$ —occur at points in the flow where the fluid velocity is downwards since for the overall correlation function to be positive $u_z < 0$. Such an asymptotics also suggests that for small Stokes numbers $\Delta_v \propto St$.

The large Stokes asymptotics, dominated by the ballistic motion of particles resulting in a short-time correlation with the fluid velocity being sampled by the particle, is more involved. However, the remarkable thing about this asymptotics is it makes a scaling prediction on Δ_v in terms of the Reynolds, Froude and Stokes numbers which are shown, through numerical simulations (Fig. 2 in Ref. [12], to be exceptionally accurate.

From the perspective of warm clouds, the nature of

setting of droplets under gravity has one further important consequence. Bec *et al.* [12] showed that gravitational settling, especially when the effect of gravity is pronounced, is accompanied by a quasi-two-dimensionalisation of the particle dynamics (Fig. 3 in Ref. [12]). A consequence of this is the estimation of the collision rate $\kappa \sim r^\gamma$ which is the average longitudinal velocity differences between pairs of same-sized particles at a separation $r \sim 2a \ll \eta$ as they approach each other. It was shown that since $\gamma = \xi_1 + D_2 - 1$, where ξ_1 is exponent of the order-1 structure function constructed from particle velocities, the approach rates must be influenced by the nature of clustering D_2 brought about through gravitational settling. Figure 4 in Ref. [12] summarises these exponents with their dependence on both the Stokes and Froude numbers and shows how, under the influence of gravity, inter-particle approach velocities are diminished, through a renormalised effective Stokes number, as the effect of gravity begins to dominate. Indeed, these results suggest that for $30\mu m$ -sized water droplets, typical in warm clouds, collision rates are almost doubled when we factor in the interplay of both gravitational and turbulent effects on their mixing. These ideas of settling are now being extended to spheroidal particles in turbulent flows which serve as an effective model for ice crystals in colder clouds [3, 86].

The findings above are obtained at moderate Reynolds number, while the Reynolds numbers in a cloud are several orders of magnitude higher. We highlight the importance of understanding how flow structures and other features change with increasing Reynolds numbers. Moreover buoyancy effects can be important, as discussed below.

V. MICROPHYSICS WITH THERMODYNAMICS

In the previous section we discussed how turbulence affects the dynamics of droplets, in that it clusters them into portions of the flow, thus encouraging droplet collisions and merger. We assumed that droplets do not affect the turbulence. Mechanically speaking, this is a fair assumption through most stages of droplet growth. This is because water droplets are very small, and form a very dilute suspension, in that occupy only a millionth of the volume in a cloud. However, droplets can distort the turbulence that drives them through the thermodynamics associated with phase change. Some of the physics behind these effects was explained in Ravichandran and Govindarajan [79].

A. Thermodynamics of phase-change

The condensation of water vapour into water and the evaporation of liquid water into vapour (hereafter just phase-change) are governed by the Clausius-Clapeyron

law,

$$\frac{dp_s}{dT} = \frac{L_v p_s}{R_v T^2}, \quad (5)$$

where p_s is the equilibrium water vapour pressure at the temperature T , L_v is the enthalpy of vaporisation, and R_v is the gas constant for water vapour. The Clausius-Clapeyron law can be derived from the condition that the vapour-liquid system is at equilibrium at the given temperature (see, e.g. [19, Chapter 5]). This equation can be integrated assuming L_v and R_v are constants (this is a reasonable assumption) to give

$$p_s = p_s^0 \exp \left(\frac{L_v}{R_v} \left[\frac{1}{T_0} - \frac{1}{T} \right] \right). \quad (6)$$

Further approximation is possible for small temperature changes ($T_0 \approx T$) to give

$$p_s = p_s^0 \exp \left(\frac{L_v (T - T_0)}{R_v T_0^2} \right). \quad (7)$$

Due to its exponential nature, the amount of water vapour that can exist in equilibrium is a rapidly changing function of the ambient temperature; the equilibrium vapour pressure roughly doubles for every 10K increase in temperature.

While the Clausius-Clapeyron law governs the *equilibrium* vapour pressure, it says nothing about *how* this equilibrium is to be reached. Chemical reactions or changes of phase that are thermodynamically favoured may nevertheless not occur because the reactions have high energies of activation. As a result, pockets of air with higher concentrations of water vapour than given by equation 6 are very commonly found in the atmosphere. The system of air and water vapour is then said to be ‘supersaturated’. In fact a cloud is often on average supersaturated. So excess water vapour is available, which can then condense. However, thermodynamically for spontaneous condensation, i.e., condensation without any pre-existing nucleation site, we need about 400% supersaturation, whereas such supersaturation is impossible under atmospheric conditions, where it is almost never greater than 5%. We therefore need cloud condensation nuclei on which condensation can occur, and droplets and aerosol particles provide such surfaces. These nuclei are typically small particles of salt or dust and a background concentration of these nuclei of about $100 - 1000 \text{ cc}^{-1}$ exists in the atmosphere. This number concentration is a function of how polluted the air is, typically being larger over the continents than over the ocean. This number concentration, then, also decides how supersaturated the air can be. Supersaturations for polluted air are typically 1% or lower, while higher supersaturations are seen in marine clouds (see, e.g. [76], chapter 2). Nuclei smaller than a critical size (called the Kohler radius) reach an equilibrium radius and do not grow beyond this (due to the fact that the saturation vapour pressure is a function of the

radius). Nuclei that are larger than the Kohler radius grow to become water droplets in clouds. These water droplets continue to grow by absorbing the water vapour in the atmosphere. The resulting release of the latent heat of vaporisation drives the large scale dynamics of clouds, as we sketch below.

A relation describing the rate at which the water droplets grow and consume water vapour can be derived assuming the water droplets are small enough for ventilation effects to be negligible (see [19] chapter 7, [76], chapter 13). This gives

$$a \frac{da}{dt} = \frac{s-1}{C\rho_w},$$

where $C = \mathcal{O}(10^7) \text{ ms/kg}$ is a thermodynamic constant which is a function of the ambient temperature. The rate of growth of a droplet is inversely proportional to its radius. As we have seen in section IV, this is one of the factors that makes explaining rain-formation challenging. If this relation is applied to a system of n droplets per unit volume, ignoring interactions, the rate at which the water vapour in the system is consumed is

$$\frac{d\rho_v}{dt} = -\frac{\rho_v/\rho_s - 1}{\tau_s}, \quad (8)$$

where τ_s is a time-scale and $\rho_s = p_s/(R_v T)$ is the saturation vapour density. This condensation of vapour results in the heating of the flow at a rate

$$\frac{dT}{dt} = \frac{L_v}{C_p} \left(\frac{\rho_v/\rho_s - 1}{\tau_s} \right).$$

The latent heat of vaporisation, $L_v \approx 2.5 \times 10^6 \text{ J/kg/K}$ is a large value. As a result of this, despite the small amounts by weight of water vapour and liquid found in clouds (typical values are $\mathcal{O}(1-10) \text{ g/kg}$), the amounts of heat released are enormous and can be $\mathcal{O}(\text{MW}/\text{m}^3)$ (see, e.g. the discussion in [66] on typical heating rates in clouds). The heating thus provided increases the temperature, and the resulting buoyancy drives the upward flow of the cloud. Differential heating of regions of the flow and the resulting buoyancy differences drive the turbulence in the flow. We look next at how particle inertia, phase change and buoyancy interact in clouds.

B. Interactions of particle inertia, thermodynamics, and buoyancy-driven flow

We refer again to the box-diagram in fig. 1 showing the different interacting phenomena in clouds. All clouds are composed of water vapour, water droplets, and aerosol particles suspended in turbulent flow. Particle inertia, phase-change, and buoyancy-driven turbulent flow are all active in clouds. However, depending on the type of cloud and the range of parameters, simplifying approximations may be made which ignore one or more of these effects. We discuss some relevant examples below which illustrate this.

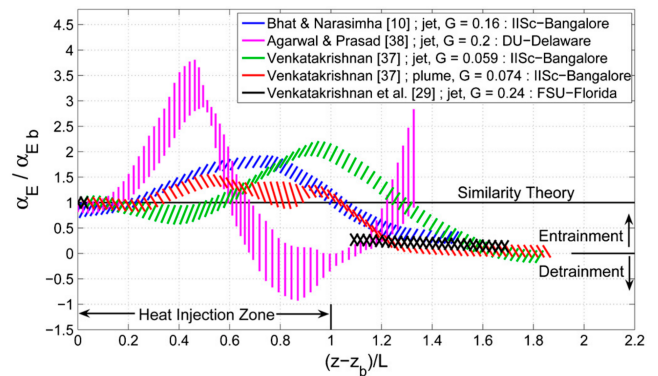


FIG. 8. The entrainment coefficient in heated plumes first increases and then decreases to zero (i.e. the plume stops entraining). Reproduced from [66].

1. Cumulus clouds: phase-change+buoyancy+turbulence

Cumulus clouds are tall, heap-like clouds found in the atmosphere, and are crucial to the maintenance of heat and mass balance in the atmosphere. Their importance in the dynamics of the atmosphere has long been recognised, with competing attempts to model them as various free-shear flows like jets, plumes, or thermals ([98, 100]). These clouds, driven by the release of latent heat in the flow, differ significantly in their dynamics from jets and plumes without such latent heating, and have been an object of study for 60 years. A fuller review of these efforts may be found in [29]. The parameter of interest in the study of these clouds is the entrainment rate—the rate at which the cloud drags in ambient (dry) air from its environment. Entrainment dilutes the cloud, leading to its ultimate demise. Entrainment in free-shear flows is still a topic of active research, and the addition of volumetric (i.e. not at the source on the ground) heating complicates the picture.

Progress has been made through laboratory experiments on cumulus clouds, showing the role of the latent heat release, reported by [66], building on work in [15, 105, 106]. The addition of latent heat to the flow seems to not only accelerate the flow but to shut down the entrainment of ambient air into the bulk of the flow. This shutdown of entrainment (shown in figure 8) is argued to be because the heating disrupts the coherent structures in the shear layer of the flow ([15, 66]). This then leads to the cloud remaining undiluted for longer and reaching higher altitudes than if the flow were a pure plume or jet.

As we have argued, the heating in the cloud arises out of the condensation of water vapour onto liquid water droplets in the cloud, and thus a full description of the dynamics would include all the phenomena listed in figure 1. However, especially for growing cumulus clouds which have not reached the precipitating state, the droplet size may be assumed to be small enough that the particle inertia is negligible. This is a reasonable as-

sumption since the size distribution in non-precipitating cumulus clouds peaks at $10\mu\text{m}$. This being the case, the droplet inertia is small and the droplets follow the velocity of the fluid. This in turn allows the droplets to be coarse-grained into a liquid-water field, a step that saves significant computational effort. Despite the challenges involved, progress has been made because of the simplifying assumptions discussed. Large eddy simulations of cumulus clouds showing this behaviour have been reported by [85]. Laboratory experiments of cumulus clouds have been reported by [66]. Direct numerical simulations for achievable Reynolds numbers are reported in [80].

2. Mammatus clouds: phase-change + particle settling + buoyancy

A type of cloud that is perhaps not as consequential as the cumulus clouds, but no less fascinating, is the mammatus cloud. Typically found underneath cumulonimbus anvil outflows, and therefore acting as harbingers of inclement weather. The reasons for the formation of these clouds is a matter of ongoing research, and a comprehensive review of the various proposed mechanisms may be found in [92], with follow-up studies in [54, 55]. A promising explanation involves the combination of the settling of water droplets out of the cumulonimbus anvils, their subsequent evaporation forming a layer of air below the anvil that is denser than the ambient air, and the eventual instability due to this density inversion. Unlike in section VB1, particle settling cannot be neglected. A study by [83] finds that the size of the mammatus lobes is proportional to the settling velocity (which increases for small droplet sizes like the square of the droplet size) and to the time-scale for phase-change (which is proportional to the inverse of the mean droplet size and the number concentration).

3. Droplets in clouds, redux: particle inertia+turbulence+phase-change

The phenomenon of warm-rain initiation and the droplet-growth bottleneck that has been a long-standing unsolved problem in cloud physics, as discussed in section IV. In studies focussing on the fluid mechanics of droplet collisions-coalescence, the effects of phase-change and thermodynamics are typically neglected. In the regime of interest—when droplets have grown to large enough sizes that their growth rates are small—this assumption is justifiable. For most of the lifetime of a cloud droplet, however, the thermodynamics of condensation cannot be neglected. The interactions of phase-change and particle inertia are thus relevant in the dynamics of clouds: broad droplet size distributions are important in the rapid growth of falling droplets

through coalescence with smaller droplets.

A first step in understanding the interactions of particle inertia and thermodynamics was taken by [96] who study how droplets interact with vortices. Clouds, being turbulent flows, are a tangle of strong vortices. Vortices, then, are suitable models for idealised studies. As we have seen in section IV, vortices expel inertial particles. When these inertial particles are also nuclei for condensation, the cores of vortices are voided of nuclei for condensation and therefore have higher vapour concentrations than the outside. [96] argue that this should have two consequences: first, that any droplets that remain trapped in the vortical region will end up experiencing larger-than-average supersaturations, and thus be able to grow to sizes not predicted by only considering cloud-average values of supersaturation; second, that the supersaturations produced in the cores of the vortices should lead to the nucleation of condensation nuclei well above cloud-base, which allows a broadening of the droplet size distributions (on the lower side). The use by [96] of this mechanism in explaining warm-rain initiation has been questioned in the literature (see [40, 102, 103]), but the central message that particle inertia and thermodynamics interact in complex ways remains relevant, in our view.

Clouds are, as we have seen, turbulent flows where the turbulence is driven by the energy provided by condensing water vapour. While large velocities can be generated by large values of buoyancy, turbulence itself, as we have also argued, is generated by *spatial inhomogeneities* in the heating. [79] propose a model of how this can be achieved starting from initially homogeneous conditions, thereby providing a route by which turbulence can sustain itself by ‘feeding’ on the latent heat of vaporisation. The mechanism builds on the aforementioned effect of inertial particles being centrifuged out of vortical regions. This leaves the vortices more supersaturated (as in [96], but keeping track of temperature changes), but also colder than their surroundings which have been heated by the condensation of water vapour. The resulting density inhomogeneities lead to baroclinic torques which generate vorticity and thus turbulence in the flow. We mention in passing that the buoyant vortices that result have interesting dynamics of their own (see [82]).

Growing clouds are also a class of free-shear flows. The edges of clouds, where the shear layers separate saturated regions from unsaturated regions, are thus regions of large inhomogeneities in vapour and droplet concentration. This results in the generation of strong sustained turbulent flow. [57–59] study this dynamics in an idealised setup where the temperature is held constant, but water droplets are allowed to grow or shrink in response to local conditions. The authors argue that, as a consequence of the high flow Reynolds numbers in a cloud, the mixing of dry ambient air with the saturated cloudy air will be highly inhomogeneous:

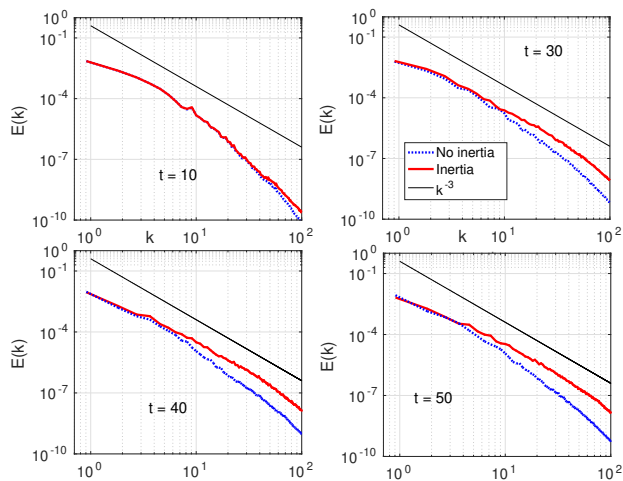


FIG. 9. The energy density $E(k)$ vs the wavenumber k in simulations with and without accounting for the effects of particle inertia. The addition of particle inertia effects provides a route for the transfer of energy to smaller scales starting from homogeneous conditions. Similar to a figure in [79]

i.e. that parcels of saturated air and parcels of subsaturated air will often be found close to each other. As a result, particles in the shear layer can have complicated growth histories; the size distribution of such droplets will also be very broad as a result. They quantify this inhomogeneity in terms of a Damkohler number which is a ratio of the time-scale of phase-change to a characteristic timescale of the flow. For large Damkohler numbers, which would be expected in the high-Reynolds number flows in the shear layers of clouds, they show that using a large Damkohler number $Da \gg 1$ results in highly skewed tails with a large number of droplets that begin at the edge of the shear layer experiencing extreme evaporation and thus shrinking significantly, while droplets in the saturated core of the flow grow slightly. In the later stages of a cloud's evolution, as large droplets formed in the cloud settle out of the cloud, they are likely to encounter these smaller droplets. The efficiency of collisions being significantly greater if the droplet sizes are different, the presence of much smaller droplets in the shear-layers could play a crucial role in rain formation.

More recently, the entire process of rain formation from monodisperse cloud droplets has been studied by [38, 87]. The authors develop a moving box model where they account for the upward velocity of a cloud by changing the mean background properties seen by the box. This allows them to follow a subvolume of the cloud as it ascends upwards. The cloud droplets initially grow by condensation of vapour. These cloud droplets eventually lead to a small number of larger droplets by collisions with each other. This is a weak effect, since collisions of similarly-sized

particles are rare. The larger droplets that eventually form start to settle at significant velocities, and grow rapidly because of collisions-coalescence with the smaller droplets. The authors report that the intensity of the turbulence (which is artificially chosen instead of plays a key role in the collisions-coalescence process, in line with expectations from work on the problem over the last two decades.

CONCLUSION AND FUTURE DIRECTIONS

The fluid dynamics of clouds is only part—if the most complex part—of climate science. We have argued here that understanding the dynamics is important in the face of the uncertainties of climate change. We hope to have convinced readers of the immense challenges and opportunities the field presents, both as an exercise in scientific curiosity and because of the far-reaching implications. Both these facets arise from the range of length- and time-scales present in the dynamics. The approach we favour—of understanding the parts in service of understanding the whole—has led to several semi-independent programmes of research which have to be eventually be united. Under present computational limitations the goal of these studies is to be able to parameterise the dynamics and improve global climate models.

Some areas of active research where the questions are reasonably well-defined and can be addressed computationally are a) A fuller understanding of entrainment in free-shear flows in general, and cloud-flows in particular. Open problems include the magnitude of the entrainment and the details of the process by which volumetric heating alters the entrainment; by extension, entrainment in merging plumes/cumulus clouds as a way of understanding the dynamics of convective aggregation; and the incorporation of the resultant better models for entrainment into global climate simulations: perhaps by extending super-parameterisation method (see [77]). b) Droplet-resolved simulations for collision-coalescence, in order to overcome limitations of the geometric collisions approach; to include effects of droplet splintering, droplet interactions, and flow-droplet coupling; and to include effects of differences in liquid/gas properties like density, temperature, conductivity in the phase-change process.

ACKNOWLEDGEMENTS

SR is supported under Swedish Research Council grant no. 638-2013-9243. JRP acknowledges funding from the IITB-IRCC seed grant. SSR acknowledges DST (India) project MTR/2019/001553 for support. RG and SSR acknowledge support of the DAE, Govt. of India, under project no. 12-R&D-TFR-5.10-1100.

-
- [1] D. Abma, T. Heus, and J.-P. Mellado. Direct Numerical Simulation of Evaporative Cooling at the Lateral Boundary of Shallow Cumulus Clouds. *Journal of the Atmospheric Sciences*, 70(7):2088–2102, 2013. ISSN 0022-4928. doi:10.1175/JAS-D-12-0230.1. URL <http://journals.ametsoc.org/doi/abs/10.1175/JAS-D-12-0230.1>.
 - [2] L. Agasthya, J. R. Picardo, S. Ravichandran, R. Govindarajan, and S. S. Ray. Understanding droplet collisions through a model flow: Insights from a burgers vortex. *Phys. Rev. E*, 99:063107, Jun 2019. doi: 10.1103/PhysRevE.99.063107. URL <https://link.aps.org/doi/10.1103/PhysRevE.99.063107>.
 - [3] P. Anand, S. S. Ray, and Ganesh Subramanian. Orientation dynamics of sedimenting anisotropic particles in turbulence. *Phys. Rev. Lett.* (in press), 2020. URL <http://arxiv.org/abs/1907.02857>.
 - [4] D. Archer. *Global warming: understanding the forecast*. John Wiley & Sons, 2011.
 - [5] P. R. Bannon. On the anelastic approximation for a compressible atmosphere. *Journal of the Atmospheric Sciences*, 53(23):3618–3628, 1996.
 - [6] J. Bec. Fractal clustering of inertial particles in random flows. *Phys. Fluids*, 15(11):L81–L84, 2003. doi: 10.1063/1.1612500.
 - [7] J. Bec. Multifractal concentrations of inertial particles in smooth random flows. *Journal of Fluid Mechanics*, 528:255–277, 2005. doi:10.1017/S0022112005003368.
 - [8] J. Bec, A. Celani, M. Cencini, and S. Musacchio. Clustering and collisions of heavy particles in random smooth flows. *Phys. Fluids*, 17(7):073301, 2005. doi: 10.1063/1.1940367. URL <https://doi.org/10.1063/1.1940367>.
 - [9] J. Bec, L. Biferale, M. Cencini, A. Lanotte, S. Musacchio, and F. Toschi. Heavy particle concentration in turbulence at dissipative and inertial scales. *Phys. Rev. Lett.*, 98:084502, Feb 2007. doi: 10.1103/PhysRevLett.98.084502.
 - [10] J. Bec, L. Biferale, M. Cencini, A.S. Lanotte, and F. Toschi. Intermittency in the velocity distribution of heavy particles in turbulence. *J. Fluid Mech.*, 646: 527–536, 2010.
 - [11] J. Bec, S. Musacchio, and S. S. Ray. Sticky elastic collisions. *Phys. Rev. E*, 87:063013, Jun 2013. doi:10.1103/PhysRevE.87.063013. URL <https://link.aps.org/doi/10.1103/PhysRevE.87.063013>.
 - [12] J. Bec, H. Homann, and S. S. Ray. Gravity-driven enhancement of heavy particle clustering in turbulent flow. *Phys. Rev. Lett.*, 112:184501, May 2014. doi: 10.1103/PhysRevLett.112.184501. URL <https://link.aps.org/doi/10.1103/PhysRevLett.112.184501>.
 - [13] J. Bec, S. S. Ray, E.-W. Saw, and H. Homann. Abrupt growth of large aggregates by correlated coalescences in turbulent flow. *Phys. Rev. E*, 93:031102, Mar 2016. doi:10.1103/PhysRevE.93.031102. URL <https://link.aps.org/doi/10.1103/PhysRevE.93.031102>.
 - [14] G. P. Bewley, E.-W. Saw, and E. Bodenschatz. Observation of the sling effect. *New J. Phys.*, 15(8):083051, 2013. URL <http://stacks.iop.org/1367-2630/15/i=8/a=083051>.
 - [15] G. S. Bhat and R. Narasimha. A volumetrically heated jet: large-eddy structure and entrainment characteristics. *Journal of Fluid Mechanics*, 325:303–330, 1996.
 - [16] A. Bhatnagar, K. Gustavsson, B. Mehlig, and D. Mitra. Relative velocities in bidisperse turbulent aerosols: Simulations and theory. *Phys. Rev. E*, 98:063107, Dec 2018.
 - [17] A. Bhatnagar, K. Gustavsson, and D. Mitra. Statistics of the relative velocity of particles in turbulent flows: Monodisperse particles. *Phys. Rev. E*, 97:023105, Feb 2018.
 - [18] E. Bodenschatz, S.P. Malinowski, R.A. Shaw, and F. Stratmann. Can we understand clouds without turbulence? *Science*, 327:970–971, 2010.
 - [19] C. F. Bohren and B. A. Albrecht. *Atmospheric Thermodynamics*. Oxford University Press, 1998. ISBN 9780195099041. URL https://books.google.nl/books?id=SSJJ_RWJGe8C.
 - [20] S. Bony, B. Stevens, D. M. W. Frierson, C. Jakob, M. Kageyama, R. Pincus, T. G. Shepherd, S. C. Sherwood, A. P. Siebesma, A. H. Sobel, M. Watanabe, and M. J. Webb. Clouds, circulation and climate sensitivity. *Nature Geoscience*, 8(4):261–268, 2015.
 - [21] J. M. Burgers. *Advances in Applied Mechanics*. Academic, New York, 1948, 1948.
 - [22] C. Canuto, M. Y. Hussaini, A. Quarteroni, and T. A. Zang. *Spectral methods: fundamental in single domains*. Springer-Verlag, Berlin, 2006.
 - [23] J. Chun, D. L. Koch, S. L. Rani, A. Ahluwalia, and L. R. Collins. Clustering of aerosol particles in isotropic turbulence. *J. Fluid Mech.*, 536:219–251, 2005. doi: 10.1017/S0022112005004568.
 - [24] P. A. Davidson. *Turbulence: An Introduction for Scientists and Engineers*. Oxford University Press, UK, 2004. ISBN 019852949X, 9780198529491.
 - [25] P. A. Davidson, Y. Kaneda, and K. R. Sreenivasan. *Ten chapters in turbulence*. Cambridge University Press, 2012.
 - [26] A. de Lozar and J.-P. Mellado. Direct numerical simulations of a smoke cloud–top mixing layer as a model for stratocumuli. *Journal of the Atmospheric Sciences*, 70(8):2356–2375, 2013.
 - [27] A. de Lozar and J.-P. Mellado. Mixing driven by radiative and evaporative cooling at the stratocumulus top. *Journal of the Atmospheric Sciences*, 72:4681, 2015.
 - [28] A. de Lozar and J.-P. Mellado. Reduction of the entrainment velocity by cloud droplet sedimentation in stratocumulus. *Journal of the Atmospheric Sciences*, 74(3):751–765, 2017.
 - [29] W. C. De Rooy, P. Bechtold, K. Fröhlich, C. Hohenegger, H. Jonker, D. Mironov, A. P. Siebesma, J. Teixeira, and J.-I. Yano. Entrainment and detrainment in cumulus convection: An overview. *Quarterly Journal of the Royal Meteorological Society*, 139(670):1–19, 2013.
 - [30] P. Deepu, S. Ravichandran, and R. Govindarajan. Caustics-induced coalescence of small droplets near a vortex. *Phys. Rev. Fluids*, 2(2):024305, 2017.
 - [31] B. J. Devenish, P. Bartello, J.-L. Brenguier, L. R. Collins, W. W. Grabowski, R. H. A. IJzermans, S. P. Malinowski, M. W. Reeks, J. C. Vassilicos, L.-P. Wang, and Z. Warhaft. Droplet growth in warm turbulent

- clouds. *Quarterly Journal of the Royal Meteorological Society*, 138(667):1401–1429, 2012.
- [32] S. Douady, Y. Couder, and M. E. Brachet. Direct observation of the intermittency of intense vorticity filaments in turbulence. *Phys. Rev. Lett.*, 67:983–986, 1991.
- [33] Y. Dubief and F. Delcayre. On coherent-vortex identification in turbulence. *J. Turbul.*, 1:N11, 2000.
- [34] D. R. Durran. Improving the anelastic approximation. *Journal of the atmospheric sciences*, 46(11):1453–1461, 1989.
- [35] G. Falkovich and A. Pumir. Sling effect in collisions of water droplets in turbulent clouds. *J. Atmos. Sci.*, 64:4497–4505, 2007.
- [36] G. Falkovich, A. Fouxon, and M.G. Stepanov. Acceleration of rain initiation by cloud turbulence. *Nature*, 419:151–154, 2002.
- [37] J.D. Gibbon, A.S. Fokas, and C.R. Doering. Dynamically stretched vortices as solutions of the 3d navier-stokes equations. *Physica D*, 132(4):497 – 510, 1999. ISSN 0167-2789.
- [38] T. Gotoh, T. Suehiro, and I. Saito. Continuous growth of cloud droplets in cumulus cloud. *New Journal of Physics*, 18(4):043042, 2016.
- [39] W. W. Grabowski. Extracting microphysical impacts in large-eddy simulations of shallow convection. *Journal of the Atmospheric Sciences*, 71(12):4493–4499, 2014.
- [40] W. W. Grabowski and P. Vaillancourt. Comments on “Preferential concentration of cloud droplets by turbulence: effects on the early evolution of cumulus cloud droplet spectra”. *Journal of the atmospheric sciences*, 56(10):1433–1436, 1999.
- [41] W. W. Grabowski and L.-P. Wang. Growth of cloud droplets in a turbulent environment. *Annual Review of Fluid Mechanics*, 45(1):293–324, 2013.
- [42] M. Gupta, P. Chaudhuri, J. Bec, and S. S. Ray. Turbulent route to two-dimensional soft crystals, 2018. URL <http://arxiv.org/abs/1812.06487>.
- [43] K. Gustavsson and B. Mehlig. Distribution of relative velocities in turbulent aerosols. *Phys. Rev. E*, 84:045304, Oct 2011.
- [44] K. Gustavsson and B. Mehlig. Distribution of velocity gradients and rate of caustic formation in turbulent aerosols at finite kubo numbers. *Phys. Rev. E*, 87:023016, 2013.
- [45] K. Gustavsson and B. Mehlig. Statistical models for spatial patterns of heavy particles in turbulence. *Adv. in Phys.*, 65(1):1–57, 2016. doi: 10.1080/00018732.2016.1164490.
- [46] K. Gustavsson, B. Mehlig, M. Wilkinson, and V. Uski. Variable-range projection model for turbulence-driven collisions. *Phys. Rev. Lett.*, 101:174503, 2008.
- [47] G. Hernandez-Duenas, A. J. Majda, L. M. Smith, and S. N. Stechmann. Minimal models for precipitating turbulent convection. *Journal of Fluid Mechanics*, 717:576–611, 2013.
- [48] P. J. Ireland, A. D. Bragg, and L. R. Collins. The effect of reynolds number on inertial particle dynamics in isotropic turbulence. part 1. simulations without gravitational effects. *J. Fluid Mech.*, 796:617–658, 2016. doi: 10.1017/jfm.2016.238.
- [49] T. Ishihara, Y. Kaneda, M. Yokokawa, K. Itakura, and A. Uno. Small-scale statistics in high-resolution direct numerical simulation of turbulence: Reynolds number dependence of one-point velocity gradient statistics. *J. Fluid Mech.*, 592:335–366, 2007. doi: 10.1017/S0022112007008531.
- [50] M. James and S. S. Ray. Enhanced droplet collision rates and impact velocities in turbulent flows: The effect of poly-dispersity and transient phases. *Sci. Rep.*, 7(1):12231, 2017.
- [51] D. Jarecka, W. W. Grabowski, and H. Pawlowska. Modeling of subgrid-scale mixing in large-eddy simulation of shallow convection. *Journal of the Atmospheric Sciences*, 66(7):2125–2133, 2009.
- [52] J. Jiménez and A. A. Wray. On the characteristics of vortex filaments in isotropic turbulence. *J. Fluid Mech.*, 373:255–285, 1998. ISSN 00221120. doi: 10.1017/S0022112098002341.
- [53] P. Kailasnath, K. R. Sreenivasan, and G. Stolovitzky. Probability density of velocity increments in turbulent flows. *Phys. Rev. Lett.*, 68:2766–2769, 1992.
- [54] K. M. Kanak and J. M. Straka. An idealized numerical simulation of mammatus-like clouds. *Atmospheric Science Letters*, 7(1):2–8, 2006.
- [55] K. M. Kanak, J. M. Straka, and D. M. Schultz. Numerical simulation of mammatus. *Journal of Atmospheric Sciences*, 65:1606, 2008.
- [56] A. B. Kostinski and R. A. Shaw. Fluctuations and luck in droplet growth by coalescence. *Bull. Amer. Meteor.*, 86(2):235–244, 2005.
- [57] B. Kumar, F. Janetzko, J. Schumacher, and R. A. Shaw. Extreme responses of a coupled scalar-particle system during turbulent mixing. *New Journal of Physics*, 14(11):115020, 2012.
- [58] B. Kumar, J. Schumacher, and R. A. Shaw. Cloud microphysical effects of turbulent mixing and entrainment. *Theor. Comput. Fluid Dyn.*, 27(3-4):361–376, jun 2013. ISSN 0935-4964. doi:10.1007/s00162-012-0272-z. URL <http://link.springer.com/10.1007/s00162-012-0272-z>.
- [59] B. Kumar, J. Schumacher, and R. A. Shaw. Lagrangian mixing dynamics at the cloudy-clear air interface. *Journal of the Atmospheric Sciences*, 71(7):2564–2580, 2014.
- [60] A. G. Lamorgese, D. A. Caughey, and S. B. Pope. Direct numerical simulation of homogeneous turbulence with hyperviscosity. *Phys. Fluids*, 17(1):015106, 2005.
- [61] A. S. Lanotte, A. Seminara, and F. Toschi. Cloud droplet growth by condensation in homogeneous isotropic turbulence. *Journal of the Atmospheric Sciences*, 66(6):1685–1697, 2009.
- [62] M. R. Maxey and J. J. Riley. Equation of motion for a small rigid sphere in a nonuniform flow. *Phys. Fluids*, 26:883, 1983.
- [63] J. Meibohm, L. Pistone, K. Gustavsson, and B. Mehlig. Relative velocities in bidisperse turbulent suspensions. *Phys. Rev. E*, 96:061102, Dec 2017.
- [64] D. Mitra and P. Perlekar. Topology of two-dimensional turbulent flows of dust and gas. *Physical Review Fluids*, 3(4):044303, 2018.
- [65] R. Monchaux, M. Bourgoin, and A. Cartellier. Analyzing preferential concentration and clustering of inertial particles in turbulence. *Int. J. Multiph. Flow*, 40:1 – 18, 2012. ISSN 0301-9322.
- [66] R. Narasimha, S. S. Diwan, S. Duvvuri, K. R. Sreenivas, and G. S. Bhat. Laboratory simulations show diabatic heating drives cumulus-cloud evolution and entrainment. *Proceedings of the National Academy of Sciences*, 108(39):16164–16169, 2011.

- [67] N.T. Ouellette, H. Xu, M. Bourgoin, and E. Bodenschatz. An experimental study of turbulent relative dispersion models. *New J. Phys.*, 8:109, 2006.
- [68] R. Pandit, P. Perlekar, and S. S. Ray. Statistical properties of turbulence: An overview. *Pramana-Journal of Physics*, 73:157, 2009.
- [69] R. Pandit, D. Banerjee, A. Bhatnagar, M. Brachet, A. Gupta, D. Mitra, N. Pal, P. Perlekar, S. S. Ray, V. Shukla, and D. Vincenzi. An overview of the statistical properties of two-dimensional turbulence in fluids with particles, conducting fluids, fluids with polymer additives, binary-fluid mixtures, and superfluids. *Physics of Fluids*, 29(11):111112, 2017.
- [70] O. Pauluis and J. Schumacher. Idealized moist Rayleigh-Bénard convection with piecewise linear equation of state. *Communications in Mathematical Sciences*, 8(1):295–319, 2010.
- [71] O. Pauluis and J. Schumacher. Self-aggregation of clouds in conditionally unstable moist convection. *Proceedings of the National Academy of Sciences*, 108(31):12623–12628, 2011.
- [72] V. E. Perrin and H. J. J. Jonker. Preferred location of droplet collisions in turbulent flows. *Phys. Rev. E*, 89:033005, Mar 2014.
- [73] V. E. Perrin and H. J. J. Jonker. Effect of the eigenvalues of the velocity gradient tensor on particle collisions. *J. Fluid Mech.*, 792:36–49, 2016.
- [74] J. R. Picardo, L. Agasthya, R. Govindarajan, and S. S. Ray. Flow structures govern particle collisions in turbulence. *Phys. Rev. Fluids*, 4:032601, 2019.
- [75] S. G. Prasath, V. Vasan, and R. Govindarajan. Accurate solution method for the maxey-riley equation, and the effects of basset history. *Journal of Fluid Mechanics*, 868:428–460, 2019. doi:10.1017/jfm.2019.194.
- [76] H.R. Pruppacher and J.D. Klett. *Microphysics of Clouds and Precipitation*. Springer Netherlands, Dordrecht, 2010. ISBN 978-0-306-48100-0. doi:10.1007/978-0-306-48100-0_2. URL https://doi.org/10.1007/978-0-306-48100-0_2.
- [77] D. Randall, M. Khairoutdinov, A. Arakawa, and W. W. Grabowski. Breaking the cloud parameterization deadlock. *Bulletin of the American Meteorological Society*, 84(11):1547–1564, 2003.
- [78] S. Ravichandran and R. Govindarajan. Caustics and clustering in the vicinity of a vortex. *Phys. Fluids*, 27(3), 2015.
- [79] S. Ravichandran and R. Govindarajan. Vortex-dipole collapse induced by droplet inertia and phase change. *J. Fluid Mech.*, 832:745–776, 2017.
- [80] S. Ravichandran and R. Narasimha. Non-Precipitating Shallow Cumulus Clouds: Theory and Direct Numerical Simulation. *Preprint*, 2020. URL <http://arxiv.org/abs/2004.09631>.
- [81] S. Ravichandran, P. Deepu, and R. Govindarajan. Clustering of heavy particles in vortical flows: a selective review. *Sādhanā*, 42:597–605, 2017.
- [82] S. Ravichandran, H. N. Dixit, and R. Govindarajan. Lift-induced vortex-dipole collapse. *Physical Review Fluids*, 2:034702, Mar 2017. doi:10.1103/PhysRevFluids.2.034702. URL <http://link.aps.org/doi/10.1103/PhysRevFluids.2.034702>.
- [83] S. Ravichandran, Eckart Meiburg, and R. Govindarajan. Settling driven instabilities in mammatus clouds. *J. Fluid Mech. (in press)*, 2020.
- [84] D. M Romps. A direct measure of entrainment. *Journal of the Atmospheric Sciences*, 67(6):1908–1927, 2010.
- [85] D. M. Romps and Z. Kuang. Do undiluted convective plumes exist in the upper tropical troposphere? *Journal of the Atmospheric Sciences*, 67(2):468–484, 2010.
- [86] A. Roy, A. Gupta, and S. S. Ray. Inertial spheroids in homogeneous, isotropic turbulence. *Phys. Rev. E*, 98:021101, Aug 2018. doi:10.1103/PhysRevE.98.021101. URL <https://link.aps.org/doi/10.1103/PhysRevE.98.021101>.
- [87] I. Saito and T. Gotoh. Turbulence and cloud droplets in cumulus clouds. *New Journal of Physics*, 20(2):023001, 2018.
- [88] E.-W. Saw, G. P. Bewley, E. Bodenschatz, S. S. Ray, and J. Bec. Extreme fluctuations of the relative velocities between droplets in turbulent airflow. *Phys. Fluids*, 26(11):111702, 2014. doi:10.1063/1.4900848.
- [89] B. L. Sawford. Reynolds number effects in lagrangian stochastic models of turbulent dispersion. *Phys. Fluids A*, 3(6):1577–1586, 1991.
- [90] Q. Schiermeier. Physicists, your planet needs you, 2015.
- [91] T. Schneider, C. M. Kaul, and K. G. Pressel. Possible climate transitions from breakup of stratocumulus decks under greenhouse warming. *Nature Geoscience*, 12(3):163, 2019.
- [92] D. M. Schultz, K. M. Kanak, J. M. Straka, R. J. Trapp, B. A. Gordon, D. S. Zrnić, G. H. Bryan, A. J. Durant, T. J. Garrett, P. M. Klein, and D.K. Lilly. The mysteries of mammatus clouds: Observations and formation mechanisms. *Journal of the Atmospheric Sciences*, 63(10):2409–2435, 2006.
- [93] J. Schumacher and O. Pauluis. Buoyancy statistics in moist turbulent rayleigh-bénard convection. *Journal of Fluid Mechanics*, 648:509–519, 2010.
- [94] J. Schumacher, B. Eckhardt, and C. R. Doering. Extreme vorticity growth in navier-stokes turbulence. *Physics Letters A*, 374(6):861–865, 2010.
- [95] R. A. Shaw. Particle-turbulence interactions in atmospheric clouds. *Annu. Rev. Fluid Mech.*, 35:183–227, 2003.
- [96] R. A. Shaw, W. C. Reade, L. R. Collins, and J. Verlinde. Preferential concentration of cloud droplets by turbulence: Effects on the early evolution of cumulus cloud droplet spectra. *Journal of the Atmospheric Sciences*, 55(11):1965–1976, 1998.
- [97] Z. She, E. Jackson, and S. A. Orszag. Memory effects are relevant for chaotic advection of inertial particles. *Nature*, 344:226–228, 1990.
- [98] P. Squires and J. S. Turner. An entraining jet model for cumulo-nimbus updraughts. *Tellus*, 14(4):422–434, 1962.
- [99] B. Stevens. Water in the atmosphere. *Phys. Today*, 66(6):29, 2013.
- [100] H. Stommel. Entrainment of air into a cumulus cloud. *Journal of Meteorology*, 4(3):91–94, 1947.
- [101] A. Tsinober. *An informal conceptual introduction to turbulence*. Springer, New York, USA, 2009.
- [102] P. A. Vaillancourt, M. K. Yau, and W. W. Grabowski. Microscopic approach to cloud droplet growth by condensation. part i: Model description and results without turbulence. *Journal of the atmospheric sciences*, 58(14):1945–1964, 2001.
- [103] P. A. Vaillancourt, M. K. Yau, P. Bartello, and W. W. Grabowski. Microscopic approach to cloud droplet

- growth by condensation. part ii: Turbulence, clustering, and condensational growth. *Journal of the atmospheric sciences*, 59(24):3421–3435, 2002.
- [104] M. A. T. Van Hinsberg, J. H. M. Thije Boonkkamp, F. Toschi, and H. J. H. Clercx. Optimal interpolation schemes for particle tracking in turbulence. *Physical Review E*, 87(4):043307, 2013.
- [105] L Venkatakrishnan, G. S. Bhat, A. Prabhu, and R. Narasimha. Visualization studies of cloud-like flows. *Current Science*, 74(7):597–606, 1998.
- [106] L. Venkatakrishnan, G. S. Bhat, and R. Narasimha. Experiments on a plume with off-source heating: Implications for cloud fluid dynamics. *Journal of Geophysical Research: Atmospheres*, 104(D12):14271–14281, 1999.
- [107] W. H. Walton and W. C. Prewett. The production of sprays and mists of uniform drop size by means of spinning disc type sprayers. *Proc. Phys. Soc. B*, 62:341–350, 1949.
- [108] T. Weidauer, O. Pauluis, and J. Schumacher. Cloud patterns and mixing properties in shallow moist rayleigh–bénard convection. *New Journal of Physics*, 12(10):105002, 2010.
- [109] M. Wilkinson, B. Mehlig, and V. Bezuglyy. Caustic activation of rain showers. *Phys. Rev. Lett.*, 97:48501, 2006.
- [110] B. W. Zeff, D. D. Lanterman, R. McAllister, R. Roy, E. J. Kostelich, and D. P. Lathrop. Measuring intense rotation and dissipation in turbulent flows. *Nature*, 34(4):B479–B498, 2003.